

# Classical Trajectories of the Continuum States of the $\mathcal{PT}$ symmetric Scarf II potential

Anjana Sinha\*

Department of Applied Mathematics, Calcutta University, 92 A.P.C. Road, Kolkata - 700 009, INDIA

## Abstract

We apply the factorization technique developed by Kuru et. al. [Ann. Phys. **323** (2008) 413] to obtain the exact analytical classical trajectories and momenta of the continuum states of the non Hermitian but  $\mathcal{PT}$  symmetric Scarf II potential. In particular, we observe that the strange behaviour of the quantum version at the spectral singularity has an interesting classical analogue.

**Key words :** Factorization method; Classical trajectories;  $\mathcal{PT}$  symmetry; Scarf II potential; Spectral Singularity

**PACS Numbers :** 03.65.-w, 03.65.Fd, 02.20.-a

\* e-mail : anjana23@rediffmail.com , sinha.anjana@gmail.com

## I. INTRODUCTION

Non Hermitian Hamiltonians, especially those with  $\mathcal{PT}$  symmetry or space time reflection symmetry, aroused curiosity among the scientific community ever since Bender et. al. showed that one can replace the condition of Dirac Hermiticity of the Hamiltonian (viz.,  $H^\dagger = H$ ) by the  $\mathcal{PT}$  symmetry of the same (i.e.  $H^{\mathcal{PT}} = H$ ), and yet obtain real and discrete spectrum under certain conditions [1, 2]. Since then scientists have extensively studied such systems [3], with an attempt to extend the framework of conventional quantum mechanics into the complex domain [4-11]. Theoretical predictions of such systems are found in quantum field theory, mathematical, atomic and solid state physics, classical optics, etc. [12], while  $\mathcal{PT}$  symmetric optical lattices have provided the ground for experimental verification [13-20].

The study of complex classical mechanics play an important role in understanding the classical limit of complex quantum theories, as it is generally observed that quantum mechanics and classical mechanics provide profoundly different descriptions of the physical world in many cases. In an attempt to bridge this gap, several studies (both analytical and numerical) of the classical trajectories  $x(t)$  of complex Hamiltonians were taken up, and many interesting observations were reported. For example, it was found in some cases that the complex classical trajectories of a particle having real energy are closed and periodic, while those for a particle having complex energy are open and irregular [4, 8, 9]. However, this does not hold in general, as it was observed that for a special discrete set of curves in the complex-energy plane, the classical orbits are actually periodic, because of the possibility of some sort of quantization condition [6]. Additionally, attempts have even been made

to explain the concept of tunnelling with the help of classical trajectories [7].

However, all the previous studies of complex classical systems have been for bound states. In one of our previous studies, we had obtained the exact analytical classical trajectories of the bound states of the  $\mathcal{PT}$  symmetric Scarf II potential [9]. The main observation in ref. [9] was that the switching of energy values from real to complex ones at the  $\mathcal{PT}$  transition point in the quantum picture, was accompanied by the changing of the corresponding classical trajectories from closed periodic curves to open irregular ones. Naturally, our next attempt is to obtain the exact analytical classical trajectories of the scattering states of the same potential. In particular, our main aim in the present work is to see if spectral singularity in the quantum picture reveals any interesting feature in the corresponding classical version. For this purpose, we shall follow the factorization technique developed by Kuru et. al. [21]. The motivation for studying the Scarf II potential is varied —

1. The problem is exactly solvable both quantum mechanically as well as classically [9].
2. The bound state spectrum exhibits the interesting phenomenon of  $\mathcal{PT}$  phase transition at the exceptional point, where the real spectrum enters the complex domain [22].
3. The scattering state spectrum shows a spectral singularity at a single positive energy, where both reflection and transmission coefficients diverge and the eigen states are no longer linearly independent [23, 24].
4. This potential has been used to study nonlinear optical beam dynamics in a single  $\mathcal{PT}$  complex crystal [14].

The organization of the paper is as follows. In Section II, we briefly introduce the formalism ap-

plied in ref. [21], and extend the same to the complex domain. We apply it to obtain the exact analytical classical trajectories for the classical analogue of the real (Hermitian) Scarf II potential in Section III, and for the  $\mathcal{PT}$  symmetric potential in Section IV. Section V is specially devoted to the classical picture at the spectral singularity. Finally, Section VI is kept for Conclusions and Discussions.

## II. FORMALISM

This section is primarily included to make the work self-contained. To briefly discuss the formalism applied in ref. [21], we start with the one dimensional classical Hamiltonian (in units  $\hbar = 2m = 1$ )

$$H(x, p) = p^2 + V(x) \quad (1)$$

where  $V(x)$  denotes the potential, and  $x$  and  $p$  are the canonical coordinates of position and momentum, respectively, with their Poisson bracket  $\{x, p\} = 1$ . Hence, the classical particle obeys the equations of motions as given by the Hamilton's equations

$$\dot{x} = \frac{\partial H}{\partial p} = 2p \quad , \quad \dot{p} = -\frac{\partial H}{\partial x} = -V'(x) \quad (2)$$

so that  $\ddot{x} = 2\dot{p} = 2V'(x)$  which on integration gives the velocity of the particle as

$$v = \frac{dx}{dt} = \pm 2\sqrt{E - V(x)} \quad (3)$$

$E$  being its energy. While extending the formalism to the complex domain, the particle is expected to lie in the complex plain, so that the path  $x(t)$  it traces out, as well as its velocity  $v(t)$ , may take complex values. The initial conditions determine the initial velocity of the particle, and any point in the complex plane may be taken as an initial starting point [5].

Following the factorization technique of ref. [21], we assume a factorization of the Hamiltonian  $H$  in the form

$$H = A^+ A^- + \gamma(H) \quad (4)$$

In usual quantum mechanical factorizations,  $\gamma$  is the factorization constant, but in eq. (4) above,  $\gamma(H)$  may depend on  $H$ . Furthermore,  $A^\pm$  are no longer complex conjugates.  $A^\pm$  are taken to be of the form

$$A^\pm = \mp i f(x) p + \sqrt{H} g(x) + \varphi(x) + \phi(H) \quad (5)$$

so that  $A^\pm$  and  $H$  are assumed to define a deformed algebra

$$\{A^\pm, H\} = \pm i\alpha(H) A^\pm, \quad \{A^+, A^-\} = -i\beta(H) A^\pm \quad (6)$$

The unknown functions are determined by solving the following equations simultaneously

$$f(x) = \frac{2}{\alpha(H)} \left[ \varphi'(x) + g'(x) \sqrt{H} \right] \quad (7)$$

$$\begin{aligned} & f(x)V'(x) - 2f'(x)[H - V(x)] \\ &= \alpha(H) \left\{ g(x)\sqrt{H} + \varphi(x) + \phi(H) \right\} \end{aligned} \quad (8)$$

$$\begin{aligned} \beta &= 2\sqrt{H} [f'(x)g(x) - f(x)g'(x)] \\ &- \frac{1}{\sqrt{H}} g(x) [2f'(x)V(x) + f(x)V'(x)] \end{aligned} \quad (9)$$

$$\begin{aligned} &+ 4f'(x)\phi'(H) [H - V(x)] \\ &- 2f(x) [\varphi'(x) + \phi'(H)V'(x)] \end{aligned}$$

Now we construct two time dependent integrals of motion of the form

$$Q^\pm = A^\pm e^{\mp i\alpha(H)t} \quad (10)$$

so that the values of  $Q^\pm$  may be denoted by

$$q^\pm = c(E) e^{\pm i\theta_0} \quad (11)$$

where  $\theta_0$  is determined from initial conditions, and

$$c(E) = |q^\pm| = \sqrt{E - \gamma(H)} \quad (12)$$

For  $c(E)$  to be real, the expression within the square root sign must be positive. This condition gives the range of energy values for the classical particle. It is worth noting here that for bound and scattering states, the complex character of the factors  $A^\pm$  may change and the deformed algebra may also be different [21].

## III. CLASSICAL ANALOGUE OF THE REAL SCARF II POTENTIAL

This section is included to provide a direct comparison between the classical pictures of the corresponding Hermitian and  $\mathcal{PT}$  symmetric Scarf II potentials. For bound states (*i.e.*,  $E < 0$ ),  $A^\pm$  are defined as

$$A^\pm = \mp i f(x) p + \sqrt{-H} g(x) + \varphi(x) + \phi(-H) \quad (13)$$

For unbounded motion ( $E > 0$ ), putting  $\sqrt{-E} = i\sqrt{|E|}$ , changes the algebra of the Poisson bracket to

$$\{A^\pm, A_0\} = \pm i\frac{\alpha_0}{2} A^\pm, \quad \{A^+, A^-\} = i\alpha_0 A_0 \quad (14)$$

where  $A_0 = -i\sqrt{H}$ .

The final expression for  $V(x)$  should be of the form

$$V(x) = \gamma_0 \operatorname{sech}^2 \frac{\alpha_0 x}{2} + 2\delta \operatorname{sech} \frac{\alpha_0 x}{2} \tanh \frac{\alpha_0 x}{2} \quad (15)$$

We have intentionally considered the coefficient of  $\operatorname{sech}^2 \frac{\alpha_0 x}{2}$ , viz.,  $\gamma_0$ , to be positive, since the quantum mechanical  $\mathcal{PT}$  symmetric version of eq. (15) displays the interesting phenomenon of spectral singularity. We shall return to this point later, in Sections IV and V. Eq. (15), demands that in the expression for  $A^\pm$  in (13) we take the following forms of the functions  $g(x)$ ,  $\varphi(x)$ ,  $\phi(H)$ :

$$g(x) \neq 0, \quad \varphi(x) = 0, \quad \phi(H) = -i \frac{\delta}{\sqrt{H}} \quad (16)$$

Solving equations (7), (8) and (9) simultaneously, one of the possible options could be

$$g(x) = \sinh \frac{\alpha_0 x}{2}, \quad f(x) = \cosh \frac{\alpha_0 x}{2} \quad (17)$$

with

$$\alpha(H) = i\alpha_0 \sqrt{H} \quad (18)$$

Putting

$$\gamma(H) = \gamma_0 + \frac{\delta^2}{H} \quad (19)$$

in eq. (4), we obtain after some simplification, the Hermitian Scarf II potential

$$H = p^2 + \gamma_0 \operatorname{sech}^2 \frac{\alpha_0 x}{2} + 2\delta \operatorname{sech} \frac{\alpha_0 x}{2} \tanh \frac{\alpha_0 x}{2} \quad (20)$$

Hence

$$c(E) = \sqrt{E - \gamma_0 - \frac{\delta^2}{E}} \quad (21)$$

Since we are dealing with scattering states,  $E$  is always positive; therefore

$$E > \frac{\sqrt{\gamma_0^2 + 4\delta^2} + \gamma_0}{2} \quad (22)$$

The integrals of motion  $Q^\pm$ , are pure imaginary; so values of  $Q^\pm$  take the form

$$q^\pm = \mp i c(E) \exp[\mp \theta_0] \quad (23)$$

Straightforward calculations give the classical trajectories and momenta for the classical analogue of the quantum mechanical Hermitian Scarf II model as

$$x(t) = \frac{2}{\alpha_0} \sinh^{-1} \left\{ \frac{c(E)}{\sqrt{E}} \sinh \left( \theta_0 + \alpha_0 \sqrt{E} t \right) + \frac{\delta}{E} \right\} \quad (24)$$

$$p(t) = \frac{1}{\cosh \frac{\alpha_0 x}{2}} c(E) \cosh \left( \theta_0 + \alpha_0 \sqrt{E} t \right) \quad (25)$$

where  $\theta_0$  denotes the initial starting point.

In Fig. 1, we plot the Hermitian Scarf II potential as in eq. (15), and in Fig. 2, we plot the phase space trajectories for this potential, for different positive energies. Parameter values used are  $\alpha_0 = 2$ ,  $\delta = 2$ ,  $\gamma_0 = 6$ . The plot shows that as the particle comes near the barrier, its classical momentum, and hence kinetic energy, decreases, as expected.

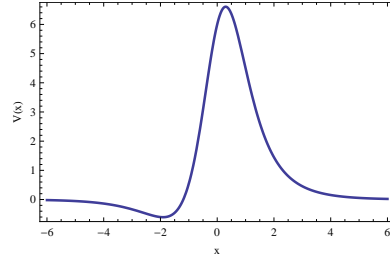


FIG. 1: Plot of  $V(x)$  against  $x$  for Real Scarf II pot.

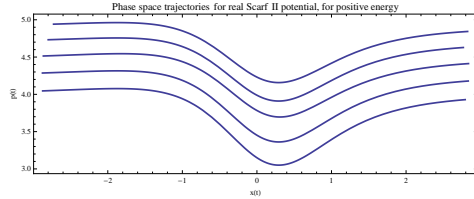


FIG. 2: Plot of  $p(t)$  against  $x(t)$  for classical analogue of Real Scarf II potential

#### IV. CLASSICAL ANALOGUE OF THE $\mathcal{PT}$ SYMMETRIC SCARF II POTENTIAL

For  $\mathcal{PT}$  symmetric Scarf II potential, we put  $\delta = i\delta_I$ , so that

$$H = p^2 + \gamma_0 \operatorname{sech}^2 \frac{\alpha_0 x}{2} + i 2 \delta_I \operatorname{sech} \frac{\alpha_0 x}{2} \tanh \frac{\alpha_0 x}{2} \quad (26)$$

For scattering states, this particular quantum mechanical model exhibits the interesting phenomenon of spectral singularity at a single positive energy  $E_s$

$$E_s = \frac{1}{4} \left[ |2\delta_I| - \left( \gamma_0 + \frac{1}{4} \right) \right] \quad (27)$$

Spectral singularity (ss) is also known as zero-width resonance, as both the transmission and reflection coefficients diverge at this particular energy. Thus these (ss) may be seen as positive energy discrete poles of transmission and reflection

coefficients. For the potential given above in eq. (26), in the quantum picture, ss occurs when the parameters  $\gamma_0$  and  $\delta_I$  satisfy the following conditions [23, 24]

$$|2\delta_I| > \gamma_0 + \frac{\text{sign of } \delta_I}{4}$$

$$\gamma_0 + |2\delta_I| = 4n^2 + 4n + \frac{3}{4}, \quad n = 0, 1, 2, \dots \quad (28)$$

The main motivation of the present study is to see if this feature is manifested in the corresponding classical picture in any way. For scattering states and hence positive energy, with

$$c(E) = \sqrt{E - \gamma_0 + \frac{\delta_I^2}{E}} \quad (29)$$

the range of energy values is obtained as

$$\text{either} \quad 0 < E < \frac{\gamma_0 - \sqrt{\gamma_0^2 - 4\delta_I^2}}{2} \quad (30)$$

$$\text{or} \quad E > \frac{\gamma_0 + \sqrt{\gamma_0^2 - 4\delta_I^2}}{2} \quad (31)$$

If the real part of the potential is greater than the imaginary part, i.e.,  $\gamma_0 > |2\delta_I|$ , then energy is always real. But in the reverse case, i.e., when the imaginary part of the potential is greater the real part ( $\gamma_0 < |2\delta_I|$ ) then energy becomes complex, with a positive real part. The interesting point to note here is that even beyond the  $\mathcal{PT}$  threshold (or phase transition point), nonlinear states can still be found in the quantum version of the Scarf II potential, with real eigenvalues [14].

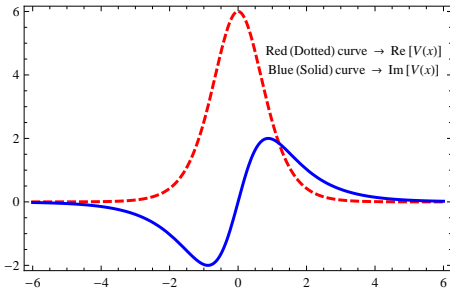


FIG. 3: Plot of  $Re V(x)$  and  $Im V(x)$  against  $x$  for the  $\mathcal{PT}$  symmetric Scarf II potential

Proceeding in a straightforward way, we obtain expressions for the classical trajectories and momenta, similar to those in equations (24) and (25), with  $\delta = i\delta_I$ ,  $c(E) = Re c(E) + i Im c(E)$ ,  $E = E_R + iE_I$ ,  $x(t) = Re x(t) + i Im x(t)$

$p(t) = Re p(t) + i Im p(t)$ , etc. In Fig. 3, we plot the potential profile of the  $\mathcal{PT}$  symmetric Scarf II Hamiltonian, for parameter values  $\alpha_0 = 2$ ,  $\delta_I = 2$ ,  $\gamma_0 = 6$ . In Figures 4, 5, 6 and 7, we plot a series of classical trajectories and momenta for this particular model, for both real and complex energy, taking the energy to lie within the permissible range, as given in equations (30) and (31).

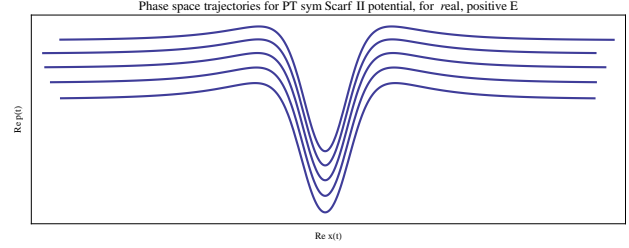


FIG. 4: Plot of  $Re p(t)$  against  $Re x(t)$  for classical analogue of  $\mathcal{PT}$  symmetric Scarf II potential, for real energy, when  $\gamma_0 > |2\delta_I|$

Fig. 4 shows the real part of the phase space trajectories for the classical analogue of the  $\mathcal{PT}$  symmetric Scarf II potential, for same parameter values as in Fig. 3 :  $\alpha_0 = 2$ ,  $\delta_I = 2$ ,  $\gamma_0 = 6$ . Analogous to the Hermitian case shown in Fig. 2, the particle slows down at the potential barrier. In both Fig. 2 and Fig. 4, the phase space curves are for different energies.

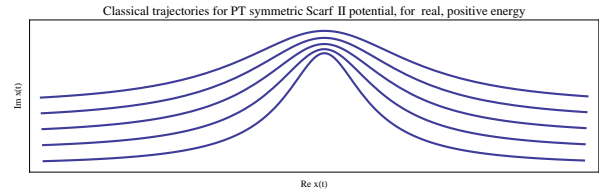


FIG. 5: Plot of  $Im x(t)$  against  $Re x(t)$  for classical analogue of  $\mathcal{PT}$  sym. Scarf II potential, for real energy

Figures 5 and 6 show the classical trajectories traced out by the particle, for real and complex energy respectively. The parameter values are  $\alpha_0 = 2$ ,  $\delta_I = 2$ ,  $\gamma_0 = 6$  ( $\gamma_0 > |2\delta_I|$ ), for the former, and  $\alpha_0 = 2$ ,  $\delta_I = 2$ ,  $\gamma_0 = 3$  ( $\gamma_0 < |2\delta_I|$ ) for the latter. The curves in Fig. 6 show a definite distortion from those in Fig. 5. Evidentially, figures 5 and 6 have no counterpart in the classical analogue of the Hermitian Scarf II model. Similar to the bound state curves of ref. [9], the initial starting point determines the trajectory, for the same energy.

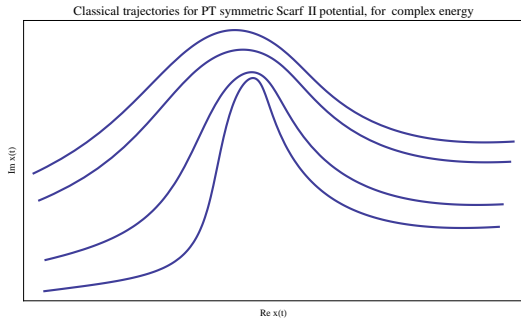


FIG. 6: Plot of  $\text{Im } x(t)$  against  $\text{Re } x(t)$  for classical analogue of  $\mathcal{PT}$  sym. Scarf II potential, for complex energy

## V. CLASSICAL PICTURE AT SPECTRAL SINGULARITY

It may be mentioned that *spectral singularities* (ss) are typical for complex scattering potentials, with no analogue in Hermitian systems. A spectral singularity of  $H$  occurs at a positive energy  $E_s = k_s^2$  in the continuous spectrum of  $H$  where the Jost solutions  $\psi_{k\pm}(x)$ , satisfying  $\psi_{k\pm}(x) \rightarrow e^{\pm ikx}$  for  $x \rightarrow \pm\infty$ ,  $E = k^2$ , become linearly dependent and their Wronskian goes to zero [24]. Thus, physically, spectral singularities correspond to scattering states that behave like zero-width resonances. Spectral singularities may be seen as positive energy discrete poles of transmission and reflection coefficients. Physical realization of spectral singularities are possible in  $\mathcal{PT}$  symmetric optical waveguides. If the frequency  $\omega$  of the incoming wave in such a waveguide can be tuned to the frequency  $\omega_s$  of the spectral singularity, then the amplitude of the outgoing wave will be considerably enhanced as  $\omega \rightarrow \omega_s$ .

To study the phenomenon of spectral singularity in the classical framework, we plot the real part of the phase space trajectories for the  $\mathcal{PT}$  symmetric Scarf II potential, in Fig. 7, for different values of real energy, but when the real part of the potential is smaller than the imaginary part, i.e.,  $\gamma_0 < |2\delta_I|$ . To be more precise, the plots are for parameter values  $\delta_I = 12$ ,  $\gamma_0 = 4$ ,  $\alpha_0 = 2$ , but for different positive energies. For this particular set of parameter values, it is observed that for low energies (as shown in the inset figures on below left), the classical particle is unable to overcome the barrier, and the phase space trajectories show a discontinuity near the potential barrier. As the energy increases the two disjoint curves come closer together, showing the inaccessible region for the classical particle decreases. Suddenly, as the energy reaches a specific value viz.,  $E_s$  (13.7 for this

particular set of parameter values), the real part of the classical momentum at the potential barrier tends to diverge. Beyond this energy, the momentum decreases with increase in energy, finally reaching a constant value. As compared to the phase space trajectories in Fig. 4 ( $\gamma_0 > |2\delta_I|$ ), these plots are inverted — the classical momentum decreases as the particle moves away from the potential barrier. We can identify this specific energy  $E_s$  as the energy at which classical spectral singularity takes place.

Thus the anomalous behaviour of a particle at the spectral singularity is found in both the quantum and classical pictures, though the manifestation is different in the two scenarios — while the reflection and transmission amplitudes blow up in the quantum picture, the real part of the momentum tends to diverge in the corresponding classical picture. This is the most important finding of the present study. Another point worth noticing here is that the condition for spectral singularity is slightly different in the quantum and classical pictures. While the quantum condition for ss is  $|2\delta_I| > \gamma_0 + \frac{1}{4}$ , the classical condition for the same turns out to be  $|2\delta_I| > \gamma_0$ . This finding is similar to the condition for exceptional point in the two pictures [9].

## VI. CONCLUSIONS

To conclude, we have studied the scattering states (having positive energy) of the classical analogue of an exactly solvable, non Hermitian quantum mechanical Hamiltonian, viz., the  $\mathcal{PT}$  symmetric Scarf II potential

$$V(x) = \gamma_0 \text{sech}^2 x - 2i\delta_I \text{sech } x \tanh x$$

by applying the factorization technique of ref. [21]. In particular, we have obtained the exact analytical classical trajectories of a particle subject to this potential, and moving about in the complex  $x$  plane. The main motivation behind this study was to see if the interesting phenomenon of spectral singularity exhibited in the quantum version at a particular energy (say  $E_s$ ), is manifested in the classical picture as well.

We plotted a series of curves, for different parameter values, for a clear picture of our findings. Figures 1 and 3 show the Hermitian and  $\mathcal{PT}$  symmetric Scarf II potentials, respectively. Fig. 2 gives the classical phase space trajectories for the former, while Fig. 4 gives the real part of the same for the latter. That the two figures resemble each other is proof of the fact that the complex  $\mathcal{PT}$  symmetric potential shares the classical features

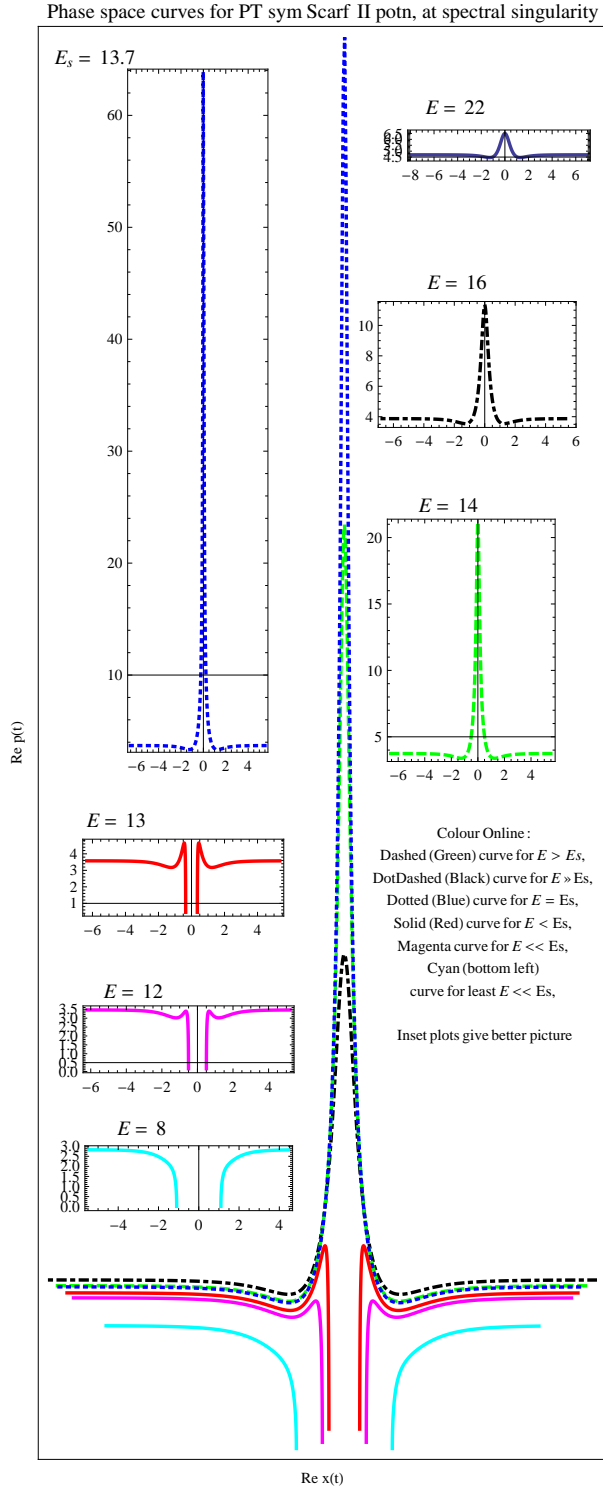


FIG. 7: Colour Online : Plot of  $Re p(t)$  against  $Re x(t)$  for classical analogue of  $\mathcal{PT}$  symmetric Scarf II potential, exhibiting spectral singularity at a single real energy  $E_s = 13.7$ , when  $\gamma_0 < |2\delta_I|$ ; Inset curves are shown for a better understanding of this phenomenon — the 3 plots on below left are for  $E < E_s$  with the bottom most curve of least  $E$ , while the 3 on upper right are for  $E > E_s$  with the topmost curve of highest  $E$

of the real (Hermitian) potential. Fig. 5 and Fig. 6 show the classical trajectories traced out by the particle ( $Im x(t)$  against  $Re x(t)$ ), in the  $\mathcal{PT}$  symmetric potential, for real and complex energy, respectively. The point to be noted here is that none of the trajectories cross each other in any plot.

Fig. 7 shows in detail the strange behaviour of the classical particle at the spectral singularity, when the imaginary part of the potential is greater than the real part, but energy is real. So long as the energy of the classical particle is sufficiently low, in fact lower than  $E_s$ , it is unable to cross the barrier, and the phase space trajectories show a discontinuity near the potential barrier. All of a sudden, at the specific energy for spectral singularity  $E_s$ , the real part of the classical momentum tends to diverge as the particle reaches the barrier. Thereafter, the particle momentum at the barrier decreases with increasing energy, thus showing a peculiar behaviour.

To give more stress to the strange behaviour of the classical momentum near and at the spectral singularity (ss), and to see how one obtains the specific energy ( $E_s$ ) at ss, we plot the real part of the classical momentum against energy, near the centre of the potential barrier, in Fig. 8, for the same set of parameter values as in Fig. 7 :  $\delta_I = 12$ ,  $\gamma_0 = 4$ ,  $\alpha_0 = 2$ . For this particular set of parameter values, the spectral singularity is found to occur in the classical picture at  $E_s = 13.7$ . As the energy approaches  $E_s$ , the momentum rises sharply, then falls rapidly with increasing energy, finally attaining a constant value for large energy.

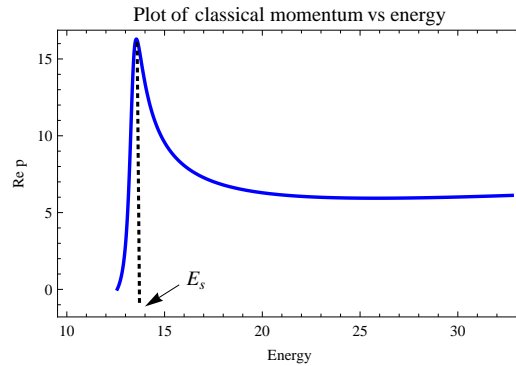


FIG. 8: Plot of  $Re p$  against  $Energy$  for classical analogue of  $\mathcal{PT}$  symmetric Scarf II potential, exhibiting spectral singularity at a single real energy  $E_s = 13.7$ , when  $\delta_I = 12$ ,  $\gamma_0 = 4$ ,  $\alpha_0 = 2$ , i.e.,  $\gamma_0 < |2\delta_I|$

In our earlier work on bound states of the  $\mathcal{PT}$  symmetric Scarf II potential [9], we had observed that at the  $\mathcal{PT}$  transition point, also known as the exceptional point, when the energy spectrum

in the quantum picture goes from the real to the complex domain, the classical trajectories switch from closed, periodic orbits to open, irregular ones. In the present study on the scattering states for the same potential, we observe that at the spectral singularity, when reflection and transmission coefficients blow up in the quantum version, the classical momentum tends to diverge. Additionally, similar to the condition for exceptional point [9], the classical condition for spectral singularity differs from the corresponding quantum condition by a factor of  $\frac{1}{4}$ .

Our next attempt would be to study more such cases, to check whether this strange behaviour of

the classical particle at the spectral singularity is characteristic of this particular potential, or some generalized conclusion can be drawn regarding the classical behaviour at the spectral singularity.

## VII. ACKNOWLEDGEMENT

Financial support for this work was provided for by the Department of Science and Technology, Govt. of India, through its grant SR/WOS-A/PS-06/2008. The author thanks Prof. P. Roy for some interesting discussions, and the unknown referee for some useful comments and suggestions.

- 
- [1] C. M. Bender and S. Boettcher, Phys. Rev. Lett. **80** (1998) 5243.
  - [2] C. M. Bender, S. Boettcher and P. Meisinger, J. Math. Phys. **40** (1999) 2201.
  - [3] For a variety of papers in this topic see the Special Issues on Conference Proceedings on *Pseudo Hermitian Hamiltonians in Quantum Physics* in link <http://gemma.ujf.cz/~znojil/conf/index.html>
  - [4] C. M. Bender, Rep. Prog. Phys. **70** (2007) 9471018.
  - [5] C. M. Bender and D. W. Darg, J. Math. Phys. **48** (2007) 042703.
  - [6] A. G. Anderson, C. M. Bender, U. I. Morone, arXiv:1102.4822 [math-ph].
  - [7] C. M. Bender, D. C. Brody, D. W. Hook, J. Phys. A : **41** (2008) 352003.
  - [8] Z. Ahmed, J. Phys. A : Math. Gen. **38** (2005) L701L706.
  - [9] A. Sinha, D. Dutta and P. Roy, Phys. Lett. A **375** (2011) 452.
  - [10] A. Nanayakkara, J. Phys. A **37** (2004) 4321.
  - [11] A. Nanayakkara, Phys. Lett. A **334** (2005) 144
  - [12] M. C. Zheng, et. al., Phys. Rev. A **82** (2010) 010103(R), *and references therein*.
  - [13] S. Longhi, Phys. Rev. A **81** (2010) 022102.
  - [14] Z. H. Musslimani, Phys. Rev. Lett. **100** (2008) 030402.
  - [15] A. Guo, et al., Phys. Rev. Lett. **103** (2009) 093902.
  - [16] C. E. Rüter, et. al, Nat. Phys. **6** (2010) 192.
  - [17] K. G. Makris et. al, Phys. Rev. Lett. **100** (2008) 103904.
  - [18] H. Ramezani et. al, Phys. Rev. A **82** (2010) 043803.
  - [19] S. Longhi, Phys. Rev. Lett. **103** (2009) 123601.
  - [20] Z. Lin, et. al, Phys. Rev. Lett **106** (2011) 213901.
  - [21] S. Kuru and J. Negro, Ann. Phys. **323** (2008) 413.
  - [22] Z. Ahmed, Phys. Lett. A **282** (2001) 343; *ibid.* Phys. Lett. A **287** (2001) 295.
  - [23] Z. Ahmed, J. Phys. A : Math. Theor. **42** (2009) 472005.
  - [24] A. Mostafazadeh, Phys. Rev. Lett. **102** (2009) 220402.